R. E. HUFFMAN and C.-I. MENG

ULTRAVIOLET IMAGING OF SUNLIT AURORAS FROM HILAT

This article reports the first successful attempt to image the global auroral display over the fully sunlit summer polar region by using the vacuum ultraviolet imager on board the recently launched HILAT satellite at an altitude of 800 km. Several daylight auroral images are presented. These images clearly demonstrate that the global auroral display can be imaged under full sunlight conditions. The earth albedo, which is the dayglow background in the ultraviolet, is not a formidable obstacle to global auroral imaging when the proper vacuum ultraviolet wavelengths are used.

INTRODUCTION

The aurora borealis (or aurora australis) is one of the most spectacular of visible natural phenomena. It occurs commonly in the polar regions, with visible observations limited to those winter nights when the sky is completely dark (even the brightest aurora is very weak, comparable to the brightness of moonlit cirrus clouds). Major advances in our understanding of auroral morphology have resulted from (a) the use of the International Geophysical Year worldwide network of more than a hundred all-sky cameras, establishing the concept of the simultaneous global scale "auroral oval" and "auroral substorm;"[1] (b) the "bird's-eye view" of global auroral activity from ISIS-2 and from the Defense Meteorological Satellite Program satellites;[2,3] and (c) the "cinematical viewing" of global auroral activity by the Dynamics Explorer-1 satellite.[4] In this article, we will present another major step: the imaging of the global auroral display over the local summer polar region. The auroras are observed under full sunlight by a vacuum ultraviolet line-scanning spectrometer imager on board the HILAT satellite.

The global auroral display is one of several manifestations of solar-terrestrial interaction; its spatial and temporal variations reveal extensive information concerning the configuration and dynamics of the magnetosphere. Since the polar auroral phenomenon is the only "visible" consequence of the solar wind/magnetosphere interaction that can be sensed remotely as opposed to in situ magnetospheric particle and field measurements, the monitoring and understanding of the global auroral display have been of major interest to geophysicists and space physicists. The observation of auroras in the sunlit hemisphere adds an important capability in understanding solar-terrestrial processes.

Auroral atmospheric emissions cover very broad wavelength ranges from infrared to extreme ultraviolet, and from long wavelength radio waves to the short wavelength bremsstrahlung X rays. In the visible and near-ultraviolet, the most intense auroral brightness can reach up to a few tens of kilo-Rayleighs per angstrom ($\overset{\circ}{A}$) while the Rayleigh scattering of the solar radiance by the atmosphere is about 10^5 kilo-Rayleighs per angstrom, making it impossible to detect optical auroral emissions. Fortunately, the atmospheric effect on solar radiation is drastically different at slightly shorter wavelengths. Radiation shorter than about $2000\,\overset{\circ}{A}$ is strongly absorbed by atmospheric molecules and atoms. Thus the corresponding solar radiation can neither penetrate the earth's atmosphere nor be reflected strongly by it. The ultraviolet background in this region in the daytime consists of resonantly scattered atomic lines (hydrogen Lyman alpha, oxygen) and airglow emission processes. The albedo from the scattering of incident solar radiation is negligible at wavelengths shorter than about $2000\,\overset{\circ}{A}$.

APPROACH

Auroral optical emission below $3000\,\overset{\circ}{A}$ was found in 1960 by a team of Johns Hopkins University scientists[5] during a sounding rocket experiment. The auroral spectrum at those wavelengths cannot be obtained from the ground because of absorption by atmospheric ozone and molecular oxygen, much in the way that the earth is protected from that part of solar radiation. Since 1960, many rocketborne and satellite spectral measurements have been made down to the approximately $300\,\overset{\circ}{A}$ limit of the extreme ultraviolet range.[6-10] The principal causes of the auroral vacuum ultraviolet and extreme ultraviolet emissions were identified as electron-excited transitions of atmospheric N_2, N, and O. In the vacuum ultraviolet range, the N_2 emissions are in the Lyman-Birge-Hopfield system with the strongest bands between 1325 and $1500\,\overset{\circ}{A}$, while the atomic oxygen transitions include the triplet near $1304\,\overset{\circ}{A}$ and the doublet near $1356\,\overset{\circ}{A}$. The Lyman alpha line of atomic hydrogen at $1216\,\overset{\circ}{A}$ is always present and is enhanced in the region of the proton aurora. Typically, the dayglow

emission features are identical in wavelength and similar in intensity.

The identification of these strong auroral emission features made it possible to use vacuum ultraviolet photometers or spectrometers to study the global morphology of the aurora, in both dark and sunlit regions, from an orbiting nadir-looking space platform. The first such experiment was performed from the OGO-4 satellite by using three broadband photometers.[11] It was clearly demonstrated that (a) vacuum ultraviolet auroral emissions are detectable in full sunlight, and (b) the maximum contrast between the aurora and dayglow background, produced by the solar ultraviolet atmospheric photoelectrons, is in the 1350 to 1550 Å band. Therefore, it should be possible to image the global auroral distribution and activity over the polar regions in both sunlit and dark hemispheres by monitoring atmospheric emissions of the proper vacuum ultraviolet wavelengths. In this article, the first successful attempt of such an experiment will be reported.

IMAGING EXPERIMENT

An experiment designed to demonstrate the feasibility and technique of global imaging of the auroral display in both dark and sunlit portions of the polar region is on board the United States Air Force Space Test Program/Defense Nuclear Agency HILAT (P83-1) satellite.[12] Launched on June 27, 1983, it is in an 830 km circular polar orbit with an inclination of 82°, producing an orbital plane precession rate of 7.6° per day. The scan mirror in the nadir-viewing position can scan 67.2° in either direction perpendicular to the satellite flight path. The light input from the mirror is focused on the entrance slit of the vacuum ultraviolet spectrometer by an off-axis parabolic telescope. The spectrometer is a 1/8 meter Ebert-Fastie type; the detector is an EMR 510G photomultiplier tube with a cesium iodide photocathode and a magnesium fluoride window. The entrance slit of the spectrometer is 1.5 millimeters, which corresponds to a spectral resolution of 30 Å; the spectrometer covers the wavelength range from about 1100 to 1900 Å. There are several advantages of using the spectrometer as the sensor of this imager instead of the more common photomultiplier tube with a filter wheel, particularly in its ability to separate nearby emission features, such as the Lyman-Borge-Hopfield bands from the oxygen lines at 1356 and 1300 Å.

With the combination of the scan mirror, the telescope, and the spectrometer, the imager can be operated in three different modes. In the imaging mode, the instrument provides global-scale imagery of atmospheric emission at a selected wavelength in the vacuum ultraviolet band. The pictorial swath is about 5000 km wide and is produced by the combination of the 3 second cross-track horizon-to-horizon scan and the forward motion of the spacecraft, resulting in a raster scan. The spatial resolution near nadir is about 20 km along the satellite track and 4 km perpendicular to it (assuming the detected vacuum ultraviolet emissions come from a 150 km altitude), but it expands to about 90 by 20 km near the horizon. There are two other modes of operation: the photometer mode and the spectrometer mode. The sensitivity of the vacuum ultraviolet instrument varies with wavelength, from about 25 Rayleighs per count per pixel for a 1300 Å emission to about 60 Rayleighs per count per pixel near 1600 Å based on the counting period per pixel used.

In addition to this vacuum ultraviolet imaging instrument, there are two nadir-pointing photometers at visible wavelengths of 3914 and 6300 Å with a 10 Å bandpass. Their field of view is a 25 km diameter circle at 100 km altitude. Data from the visible photometers are sampled about once per second. These two well-known auroral wavelengths are chosen to monitor the total energy deposition and the spectral characteristics of precipitating electrons.[13,14] The visible photometers operate only in the dark hemisphere and are controlled automatically by sensing the earth's albedo brightness.

Details of the technique used for this experiment are described in the article by Schenkel and Ogorzalek in this issue.

DAYLIGHT AURORAL IMAGERY

The auroral imagery presented here was collected over the northern hemisphere in July 1983 near the summer solstice, in contrast to the familiar winter polar-region observations. It is useful to illustrate schematically the approximate orientations of the auroral oval at the two solstices (Fig. 1). During our observations, the major part, if not all, of the northern auroral oval was under full sunlight, the most unfavorable condition in which to observe the optical auroral display. The orbital plane of the HILAT satellite is in the dawn-dusk meridian, its motion in the northern hemisphere being poleward in the dusk sector and equatorward in the dawn sector.

Figure 2 is an example of an evening pass tracked at APL on July 18, 1983, at about 2300 universal time (UT), imaging the atmospheric emission at 1356 (±15) Å over the eastern part of the North American continent and the western part of the Atlantic Ocean from Cuba to the Hudson Strait. The width of the picture covers about 4000 km. It is presented in false color with the color bar on the right indicating relative brightness from very intense (white) to no detectable signals (below 28 Rayleighs) (black). The light blue background is the dayglow emission caused by the interaction between atmospheric molecules and atoms and the photoelectrons generated by solar ultraviolet radiation. The dark blue and black on the right correspond to the transition into the dark hemisphere. The calculated geometric terminator on the earth's surface is shown for reference by a vertical dotted line. The yellow-green on the left is associated with the limb-brightening phenomenon of dayglow because of enhanced volume per solid angle as the imager field of view moves toward the horizon. The most exciting part is the observation of the evening
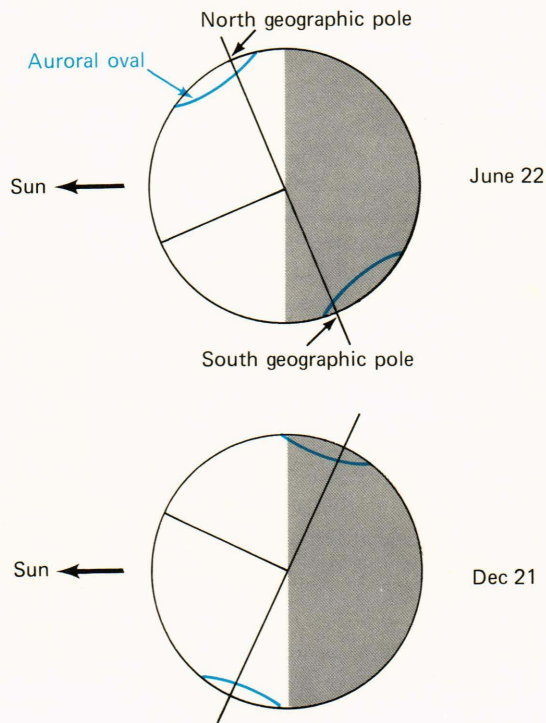
Figure 1 — The configuration of the northern and southern auroral ovals during summer and winter solstices. Note the total exposure of the northern auroral oval to the daylight in northern summer, corresponding to the auroral imagery obtained from HILAT.

Figure 2 — Image of the dayglow and the evening auroral oval at a wavelength of 1356 Å obtained over the eastern part of the North American continent on July 18, 1983. It is shown in false color (see text). The noon meridian is toward the left side of the picture.

Figure 3 — Enlarged image of the evening auroral oval with a weak westward traveling surge.

auroral oval extending across Hudson Bay; it is shown as yellow-green structures above the dayglow background. These structures are clearly identifiable even in the limb-brightening region.

The optical auroral features are detected more than 3000 km into the daylight region and are shown enlarged in Fig. 3. The main feature is a degenerated westward traveling surge, shown as a knot with two parallel arcs along the oval. The dimension of the surge is about 200 km, and the discrete arcs are about 20 km wide and approximately 20 km apart.

A morning pass on July 16, 1983, at about 1050 UT is illustrated in Fig. 4. In this picture, the dark side of the earth is on the left and is indicated by the black and dark blue. The morning auroral oval was in the sunlit hemisphere, indicated by the yellow and green band extending across southern Hudson Bay. It has the typical morning auroral oval characteristic of a diffuse aurora without significant discrete structures. The morning parts of the auroral oval over Newfoundland and to the east were viewed near the horizon from the spacecraft. The limb brightening associated with the auroral oval is clearly more intense than that of the dayglow.

The next example (Fig. 5) is an image of the major part of the auroral oval detected on July 23, 1983, at about 1500 UT. The data on this satellite pass were received at Kiruna, Sweden. It is interesting to point out that the northern geomagnetic dipole was near local noon; thus the auroral oval was tilted toward the sun and fully sunlit, a maximum daylight ex-
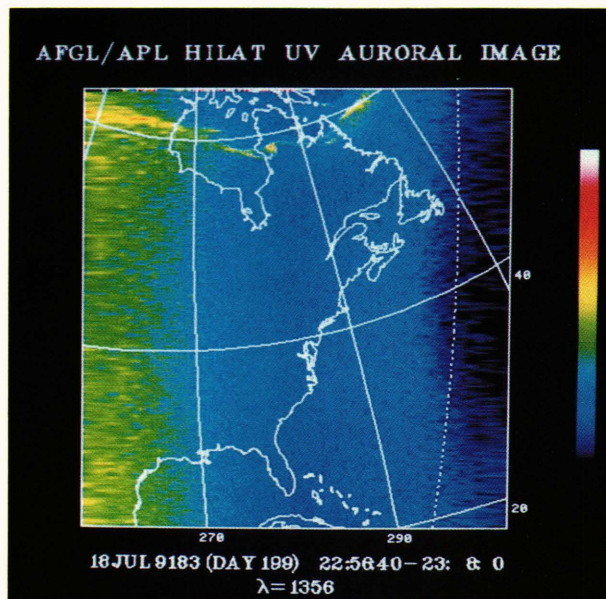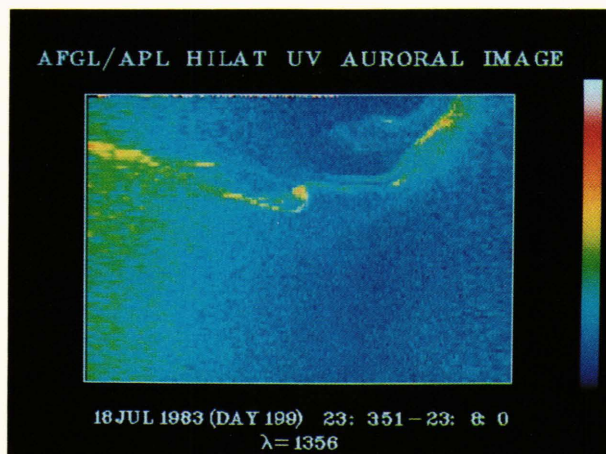
posure (i.e., a very unfavorable condition for the optical auroral observation). Even the midnight portion of the auroral oval was in daylight. The atmospheric emissions monitored were at 1493 ($\pm$15) Å. In this picture, the sun is toward the left. The auroral oval from afternoon to midnight was imaged above the dayglow background; its display indicates the progress of a weak auroral substorm. Active auroras were over central and west Siberia near the Arctic coast of the Soviet Union. Faint discrete and diffuse auroras extended along the afternoon and evening oval. These observed vacuum ultraviolet auroral features in the sunlit polar region are similar to those auroral features of the visible wavelengths commonly
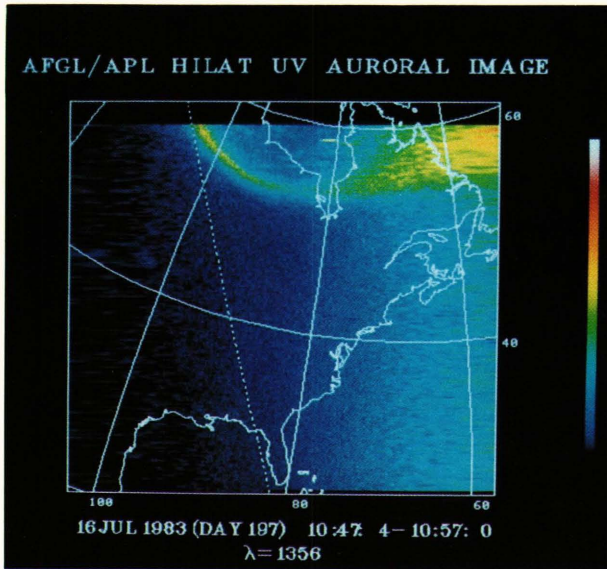
Figure 4 — Image of the dayglow and the morning auroral oval at 1356Å observed on July 16, 1983. The noon meridian is toward the right.
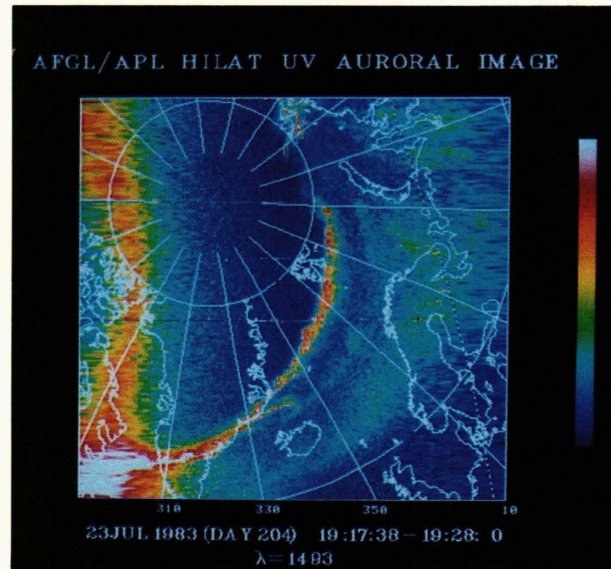

Figure 6 — Image of the sunlit auroral oval observed during the recovery phase of an auroral substorm. Note the expanded auroral oval (approximately 10° wide near midnight). The diffused feature was seen along most of the oval. The bright band on the left edge is due to the limb brightening.
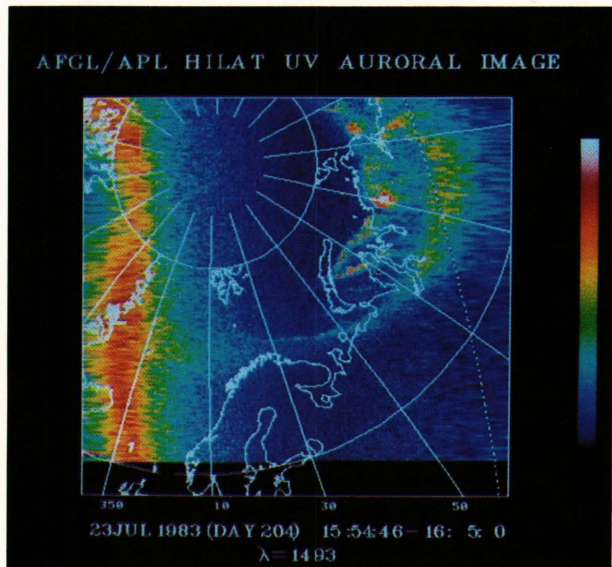

Figure 5 — Image of the auroral oval under full sunlight observed on July 23, 1983, over the northern polar region. A weak auroral substorm was in progress over the Arctic coast of Russia. The image was made at a wavelength of 1493Å.

emission of about 100 to 200 km wide, similar to the auroral morphology in the visible wavelength. The simultaneous magnetic field, electron precipitation, and electric field measurements from the HILAT satellite of this event will be discussed in companion papers in this issue. The HILAT spacecraft is the first space program to provide measurements of these complementary experiments together with the auroral imagery.

The vacuum ultraviolet imager on board the HILAT satellite clearly demonstrates that the global auroral display in the local summer hemisphere under sunlight conditions can be imaged by using properly chosen wavelengths. The earth dayglow background caused by solar radiation have prevented auroral observation in the visible and near-ultraviolet ranges. This is not a formidable obstacle to the above-described optical measurement. This first successful attempt to image the auroral display in full daylight shows that continuous and complete auroral monitoring is possible from space platforms.

observed over dark polar regions by previous spacecraft (see, for example, Refs. 2 and 3).

The last example (Fig. 6), detected on July 23, 1983, at about 1920 UT, reveals the global auroral distribution in the recovery phase of an intense magnetospheric substorm; the data were received at Kiruna, Sweden. Along the auroral oval, a band of diffuse auroral glow with irregular brighter patches is the dominant feature, and the width of the oval is over 2000 km near the midnight sector over the Siberian Arctic coast. The poleward edge of the widened auroral oval is delineated by a very bright ultraviolet

REFERENCES

[1]S.-I. Akasofu, *Polar and Magnetospheric Substorms*, D. Reidel Publishing Co., Dordrecht, Holland (1968).
[2]S.-I. Akasofu, "A Study of Auroral Displays Photographed from the DMSP-2 Satellite and from the Alaska Meridian Chain of Stations," *Space Sci. Rev.* **16**, 617 (1974).
[3]S.-I. Akasofu, "Recent Progress in Studies of DMSP Auroral Photographs," *Space Sci. Rev.* **19**, 169 (1976).
[4]L. A. Frank, J. D. Craven, J. L. Burch, and J. D. Winningham, "Polar Views of the Earth's Aurora with Dynamics Explorer," *Geophys. Res. Lett.* **9**, 1001 (1982).
[5]W. G. Fastie, H. W. Crosswhite, and T. P. Markham, "Far-ultraviolet Auroral Spectra with a Rocket Ebert Spectrophotometer," *Ann. Geophys.* **17**, 109 (1961).
[6]H. Park, P. D. Feldman, and W. G. Fastie, "The EUV (750-1230Å) Spectrum of an Aurora," *Geophys. Res. Lett.* **4**, 41 (1977).

[7] R. E. Huffman, F. J. LeBlanc, J. C. Larrabee, and D. E. Paulson, "Satellite Vacuum Ultraviolet Airglow and Auroral Observations," *J. Geophys. Res.* **85**, 2201 (1980).

[8] P. D. Feldman and E. P. Gentieu, "The UV Spectrum of an Aurora 530-1520 Å," *J. Geophys. Res.* **87**, 2453 (1982).

[9] F. Paresce, S. Chakrabarti, R. Kimble, and S. Bowyer, "The EUV Spectrum of Day and Nightside Auroras: 800-1400 Å," *J. Geophys. Res.* **88**, 4905 (1983).

[10] F. Paresce, S. Chakrabarti, R.Kimble, and S. Bowyer, "The 300-900 Å Spectrum of a Nightside Aurora," *J. Geophys. Res.* **88**, 10,247 (1983).

[11] T. A. Chubb and G. T. Hicks, "Observations of the Aurora in the Far Ultraviolet from OGO 4," *J. Geophys. Res.* **75**, 1290 (1970).

[12] The HILAT Science Team, "The HILAT Program," *EOS, Trans. Am. Geophys. Union* **64**, 163 (1983).

[13] M. H. Rees and R. A. Jones, "Time Dependent Studies of the Aurora II: Spectroscopic Morphology," *Planet. Space Sci.* **21**, 1213 (1973).

[14] R.B. Roble and M. H. Rees, "Time Dependent Studies of the Aurora: Effects of Particle Precipitation on the Dynamic Morphology of Ionospheric and Atmospheric Properties," *Planet. Space Sci.* **25**, 991 (1977).